Nuclear Engineering and Technology 52 (2020) 2918–2927

Contents lists available at ScienceDirect

Nuclear Engineering and Technology

journal homepage: www.elsevier.com/locate/net

Original Article

Simplified elastic-plastic analysis procedure for strain-based fatigue assessment of nuclear safety class 1 components under severe seismic loads

Jong-Sung Kim [a, *], Jun-Young Kim [b]

[a] Department of Nuclear Engineering, Sejong University, 209, Neungdong-ro, Gwangjin-gu, Seoul, Republic of Korea
[b] Department of Nuclear Engineering, Graduate School, Sejong University, 209, Neungdong-ro, Gwangjin-gu, Seoul, Republic of Korea

ARTICLE INFO

Article history:
Received 3 April 2020
Received in revised form
17 April 2020
Accepted 10 May 2020
Available online 16 May 2020

Keywords:
Simplified elastic-plastic analysis procedure
Severe seismic loads
Penalty factor
Fatigue assessment
Strain calculation
Nuclear safety class 1 components

ABSTRACT

This paper proposes a simplified elastic-plastic analysis procedure using the penalty factors presented in the Code Case N-779 for strain-based fatigue assessment of nuclear safety class 1 components under severe seismic loads such as safety shutdown earthquake and beyond design-basis earthquake. First, a simplified elastic-plastic analysis procedure for strain-based fatigue assessment of nuclear safety class 1 components under the severe seismic loads was proposed based on the analysis result for the simplified elastic-plastic analysis procedure in the Code Case N-779 and the stress categories corresponding to normal operation and seismic loads. Second, total strain amplitude was calculated directly by performing finite element cyclic elastic-plastic seismic analysis for a hot leg nozzle in pressurizer surge line subject to combined loading including deadweight, pressure, seismic inertia load, and seismic anchor motion, as well as was derived indirectly by applying the proposed analysis procedure to the finite element elastic stress analysis result for each load. Third, strain-based fatigue assessment was implemented by applying the strain-based fatigue acceptance criteria in the ASME B&PV Code, Sec. III, Subsec. NB, Article NB-3200 and by using the total strain amplitude values calculated. Last, the total strain amplitude and the fatigue assessment result corresponding to the simplified elastic-plastic analysis were compared with those using the finite element elastic-plastic seismic analysis results. As a result of the comparison, it was identified that the proposed analysis procedure can derive reasonable and conservative results.

1. Introduction

Nuclear safety class components should be satisfied with the requirements for all service levels limit including level A, B, C and D which are specified in the ASME (American Society of Mechanical Engineers) B&PV (Boiler and Pressure Vessels) Code, Section III [1]. Service level D includes faulted conditions such as pipe rupture loads and safety shutdown earthquake (SSE) having frequency of occurrence of less than 10^{-4}/reactor year and greater than 10^{-6}/reactor year [2]. The 1994 version of the ASME B&PV Code, Sec.III [3] considered fatigue as one of plausible failure mechanisms for the service level D, but after the version, fatigue has been not treated as the damage mechanisms to be considered until the latest version [1].

It has been reported that some beyond design-basis earthquakes (BDBEs) have occurred in nuclear power plants [4,5]. So, in response to these events, nuclear regulatory bodies such as the United States Nuclear Regulatory Commission (US NRC) and the Japanese National Security Council (NSC) issued guidelines for seismic design or re-evaluation considering BDBE and plastic strain [6,7]. In addition, the International Atomic Energy Agency (IAEA) categorized BDBE as design extended condition (DEC) [8]. The ASME B&PV Code Committee has organized working groups related to BDBE [9,10]. Recently, some studies [11-17] have performed strain-based seismic evaluation of nuclear safety class 1 components after occurrence of BDBEs. The experimental studies [11-13] identified that fatigue is a principal failure mechanism of nuclear components subject to severe seismic loads such as SSE and BDBE whereas the design codes [1] does not require fatigue assessment for the severe seismic loads. Nakamura et al. performed a series of inelastic benchmark and parametric analyses on the tests of pipe elbows and piping systems made of carbon and austenitic stainless steels to investigate reliability and variability of finite element (FE) elastic-plastic analysis [14,15]. They found that dynamic FE seismic analysis may be very sensitive to the analysis variables. Based on the inelastic benchmark and parametric

* Corresponding author.
E-mail address: kimjsbat@sejong.ac.kr (J.-S. Kim).

https://doi.org/10.1016/j.net.2020.05.008

Nomenclature

E	modulus of elasticity
K_e	penalty factor for primary stress and secondary membrane stress ranges
K_e'	overall elastic-plastic strain concentration factor
K_n	plastic strain redistribution factor in notch for secondary bending stress range caused by linear through-wall thermal gradient
K_{se}	penalty factor for primary stress and secondary membrane stress ranges caused by seismic anchor motion
K_{sn}	plastic strain redistribution factor in notch for secondary bending stress range caused by seismic anchor motion
K_{sv}	Poisson's ratio factor for secondary local stress range caused by seismic anchor motion
K_v	Poisson's ratio factor for secondary local stress range
N	number of cycles of dynamic load
Q	isotropic hardening parameter of the Chaboche hardening model
S_a	stress intensity range calculated by the combination of the terms in eqs.(2)~(4)
$S_a(N)$	allowable stress amplitude for N cycles of load
S_{alt}	alternating stress (=one-half of the stress intensity range S_a)
S_{lt}	local thermal stress intensity range
S_n	range of primary plus secondary stress intensity
S_m	design stress intensity
S_p	total stress intensity range
$S_{p\text{-}lt}$	total stress intensity range excluding local thermal stresses
$S_{p\text{-}sb\text{-}sp}$	total stress intensity range excluding the secondary bending and secondary peak stresses due to seismic anchor motion
$S_{p\text{-}sp}$	total stress intensity range excluding the secondary peak stresses due to seismic anchor motion
$S_{p\text{-}tb\text{-}lt}$	total stress intensity range excluding thermal bending and local thermal stresses
S_{sb}	secondary bending stress intensity range due to seismic anchor motion
S_{sb+sp}	secondary bending plus secondary peak stress intensity range due to seismic anchor motion
S_{sp}	secondary peak stress intensity range due to seismic anchor motion
S_{tb}	thermal bending stress intensity range
S_{tb+lt}	thermal bending plus local thermal stress intensity range
TF	triaxiality factor
A	factor to adjust the fatigue curves of Appendix I to obtain a factor of safety of 2 against failure
B	isotropic hardening parameter of the Chaboche hardening model
c_1, c_2, c_3	kinematic hardening parameters of the Chaboche hardening model
n	strain hardening exponent given in Table NB-3228.5(b)-1
m	material parameter given in Table NB-3228.5(b)-1
γ_1, γ_2, γ_3	kinematic hardening parameters of the Chaboche hardening model
ε_{xx}, ε_{yy}, ε_{zz}	normal strains in the axial directions given in each subscript
ε_{xy}, ε_{yz}, ε_{zx}	shear strains in the axial directions given in each subscript
$(\varepsilon_{alt})_{max}$	maximum total equivalent strain amplitude
$(\varepsilon_{eq})_{max}$	maximum total equivalent strain
σ_0	kinematic hardening parameter of the Chaboche hardening model
σ_1, σ_2, σ_3	principal stresses
σ_{von}	von Mises effective stress

Abbreviations

ASME	American Society of Mechanical Engineers
BDBEs	beyond design-basis earthquakes
B&PV	boiler & pressure vessels
DEC	design extended condition
E-W	east-west
FE	finite element
FEA	finite element analysis
IAEA	International Atomic Energy Agency
JSME	Japan Society of Mechanical Engineers
NSC	National Security Council
N-S	north-south
PGA	peak ground acceleration
SSE	safety shutdown earthquake
US NRC	United States Nuclear Regulatory Commission

analysis results, the Japan Society of Mechanical Engineers (JSME) issued a Code Case in the framework of JSME Nuclear Codes and Standards to incorporate a seismic design evaluation methodology for piping by means of advanced elastic-plastic response analysis methods and strain-based fatigue criteria [16]. The JSME Code Case, NN-CC-008 [16] requires strain calculation for fatigue assessment. The ASME B&PV Code Committee has been developing a Code Case Nxxx specifying alternative rules for level D service limits of class 1, 2, and 3 piping systems [17]. The Code Case proposes strain-based acceptance criteria for reversing dynamic loads (e.g., SSE) not required to be combined with non-reversing dynamic loads. However, the Code Case does not present strain and stress triaxiality calculation procedures.

Under severe seismic loads, nuclear components may be subjected to low cycle fatigue due to high load magnitude. Plastic strain may occur in the low cycle fatigue region. Elastic-plastic analysis is needed to accurately simulate plastic strain. However, elastic-plastic analysis is not only very sensitive to analysis variables but also requires much more data than elastic analysis. Hence, due to these drawbacks, nuclear industries have generally performed elastic stress analysis for various transients and then evaluated fatigue lifetime using the elastic stress analysis results. However, the elastic stress analysis cannot consider the plastic strain. Therefore, ASME B&PV Code Committee has devised a simple elastic-plastic analysis procedure to increase the stress amplitude by multiplying a penalty factor to the elastic stress analysis results. In the ASME B&PV Code, Sec.III, a prerequisite for fatigue analysis is that the primary-plus-secondary stress intensity range should not exceed $3S_m$, where S_m is the design stress intensity [1,18]. If the stress intensity range exceeds this limit, the Code provides the simplified elastic-plastic analysis approach for fatigue evaluation. The simplified elastic-plastic analysis procedure can easily calculate the alternating stress intensities considering plastic effect by means of penalty factors and elastic stress analysis results. However, the Code does not specify that the simplified elastic-plastic analysis procedure can apply to level D service limits [1,18]. Kim et al.

proposed penalty factor equations that take into consideration the weld strength over-match given in the classified form similar to the revised equations presented in the Code Case N-779 [19]. There are no technical bases specifying a simplified elastic-plastic analysis procedure applicable to fatigue assessment of level D services and no relevant studies have been conducted.

This paper presents a strain-based simplified elastic-plastic analysis procedure for fatigue assessment of nuclear safety class 1 components subjected to severe seismic loads and its application to a hot leg nozzle in pressurizer surge line under combined loading including seismic inertia load, seismic anchor motion, deadweight, and pressure. In order to derive the strain-based simplified elastic-plastic analysis procedure, the simplified elastic-plastic analysis procedure in the Code Case N-779 and the stress categories corresponding to normal operation and seismic loads were reviewed. Based on the review results, the strain-based simplified elastic-plastic analysis procedure, was proposed to calculate the total strain amplitude for strain-based fatigue assessment of nuclear safety class 1 components under severe seismic loads. A reference total strain amplitude value was determined via performing dynamic FE cyclic elastic-plastic seismic analysis for the hot leg nozzle. In addition, static FE elastic stress analyses for deadweight, pressure, and seismic anchor motion, and dynamic FE elastic stress analysis for seismic inertia load were performed for the hot leg nozzle. Then, a total strain amplitude was calculated using the proposed analysis procedure and each finite element analysis (FEA) result. Strain-based fatigue assessment was performed for the detailed analysis and the simplified elastic-plastic analysis. Validity of the proposed analysis procedure was verified via comparing the total strain amplitude and the fatigue assessment result for the simplified elastic-plastic analysis with those for the detailed FE elastic-plastic seismic analysis.

2. Proposal of stain-based simplified elastic-plastic analysis procedure

This section summarizes and analyses the simplified elastic-plastic analysis procedure and penalty factor equations presented in ASME B&PV Code, Section III, Code Case N-779. In addition, stress categories corresponding to deadweight, pressure, seismic inertia load and seismic anchor motion are classified. Finally, the section proposes a simplified elastic-plastic analysis procedure based on the analysis and classification results.

2.1. ASME B&PV code, Section III, Code Case N-779 [18]

Design fatigue curves in the ASME B&PV Code, Sec.III should be used in fatigue assessment of nuclear safety-related components. The design fatigue curves were obtained by multiplying elastic modulus by the strain amplitude-fatigue life cycle curves derived from strain-controlled fatigue tests [20]. That is, the design fatigue curves have the appearance of stress amplitude-fatigue life cycle curve, but have the nature of strain amplitude-fatigue cycle curve. Plastic strain may occur in low cycle fatigue region. The ASME B&PV Code, Sec.III introduced a simplified elastic-plastic analysis procedure including the penalty factors to reflect this plastic strain in elastic analysis results, as presented in the ASME B&PV Code, Sec.III, NB-3228.5 [21]. The simplified elastic-plastic analysis procedure is too conservative because it does not take into account differences in stress redistribution characteristics according to stress categories. In order to mitigate this excessive conservatism, the ASME B&PV Code Committee published Code Case N-779. The following requirements are given in Code Case N-779:

The $3S_m$ limit on the range of primary plus secondary stress intensity may be exceeded provided that the following rules are met:

A. The component meets the requirements of subparagraphs (a), (c), (d), (e), and (f) of NB-3228.5.
B. The value of S_{alt} used for entering the design fatigue curve is one-half of the stress intensity range S_a calculated by the combination of the terms in C, D and E below.

$$S_{alt} = 0.5S_a = 0.5(K_eS_{p\text{-}tb\text{-}lt}+K_\nu K_nS_{tb}+K_\nu S_{lt}) \quad (1)$$

$S_{p\text{-}tb\text{-}lt}$ = total stress intensity range excluding thermal bending and local thermal stresses.

S_{tb} = thermal bending stress intensity range
S_{lt} = local thermal stress intensity range

C. The total stress intensity ranges, excluding both thermal bending stress caused by linear through−wall thermal gradients and local thermal stresses, shall be multiplied by the factor K_e given in NB-3228.5(b) as follows:

$$K_e = 1.0, \text{ for } S_n \le 3S_m$$

$$= 1.0+[(1\text{-}n)/n(m\text{-}1)]\times(S_n/3S_m\text{-}1)$$

$$\text{for } 3S_m < S_n < 3mS_m$$

$$= 1/n, \text{ for } S_n \ge 3mS_m \quad (2)$$

S_n = range of primary plus secondary stress intensity.

The values of the material parameters m and n for the various classes of permitted materials are as given in Table NB-3228.5(b)-1.

D. The local thermal stress range is multiplied by a factor K_ν for Poisson's ratio effects:

$$K_\nu = 1.4, \text{ for } S_p > 3S_m \text{ and } S_{p\text{-}tb\text{-}lt} \ge 3S_m$$

$$= 1.0 + 0.4(S_p\text{-}3S_m)/(S_{tb+lt}),$$

$$\text{for } S_p > 3S_m \text{ and } S_{p\text{-}tb\text{-}lt} < 3S_m$$

$$= 1.0, \text{ for } S_p \le 3S_m \quad (3)$$

$$\text{and } K_\nu \le K_e$$

S_p = total stress intensity range
S_{tb+lt} = thermal bending plus local thermal stress intensity range

E. The thermal bending stress range caused by linear through-wall thermal gradients is multiplied by a factor K_ν as defined in (4) above for Poisson's ratio effects, and a factor K_n as defined below for plastic strain redistribution at local discontinue-ties (such as notches):

$$K_n = 1.0+\{(S_{p\text{-}lt}/S_n)^{(1-n)/(1+n)}\text{-}1\}$$

$$\{(S_{p\text{-}lt}\text{-}3S_m)/S_{p\text{-}lt}\}, \text{ for } S_{p\text{-}lt} > 3S_m$$

$$= 1.0, \text{ for } S_{p\text{-}lt} \le 3S_m \quad (4)$$

$$\text{and } K_n\times K_\nu \le K_e$$

$S_{p\text{-}lt}$ = total stress intensity range exclude-ing local thermal stresses

F. As an alternative to (2) through (5) above, an overall elastic-plastic strain concentration factor K_e' can be deter-mined directly from an elastic-plastic analysis of the component and the load case under consideration. K_e' is defined as the ratio of the numerically maximum principal strain range from the elastic-plastic analysis to that from the elastic analysis. The resulting K_e' can be applied to other load cases with an elastically predicted stress range less than or equal to the elastic stress range of the load case used to derive K_e'. The value of S_{alt} used for entering the design fatigue curve is multiplied by K_e'.

K_e, K_ν, and K_n all represent penalty factors. K_e is the penalty factor for primary stress and secondary membrane stress ranges. K_ν is the penalty factor that takes into consideration the Poisson's ratio effect for secondary local stress range. K_n is the penalty factor that considers the plastic strain redistribution effect in a notch for secondary bending stress range caused by linear through-wall thermal gradient.

From eq. (1), it can be identified that K_e is multiplied by total stress intensity range excluding thermal bending and local thermal stresses, $K_n \times K_\nu$ is multiplied by thermal bending stress intensity range, and K_ν is multiplied by local thermal stress intensity range. From eqs. (2)~(4), it can be found that K_e is a function of primary plus secondary stress intensity range, K_ν is a function of total stress intensity range, thermal bending plus local thermal stress intensity range, and total stress intensity range excluding thermal bending and local thermal stresses, and K_n is a function of primary plus secondary stress intensity range and total stress intensity range excluding local thermal stresses. Thermal stresses can be classified as secondary stress having the basic characteristics of self-limiting. That is, thermal bending stresses and local thermal stresses can be classified as secondary bending stress and secondary peak stress, respectively.

2.2. Strain-based simplified elastic-plastic analysis procedure

Seismic events may occur during the normal operation state with deadweight and pressure. In addition, the seismic loads can be classified into seismic inertia load and seismic anchor motion. Deadweight, pressure and seismic inertia load are classified as primary stress having the basic characteristics of not self-limiting, while seismic anchor motion has the basic characteristics of secondary stress being self-limiting.

Replacing the thermal bending and local thermal stress terms in the simplified elastic-plastic analysis procedure in the ASME B&PV Code, Sec.III, Code Case N-779 with secondary bending and secondary peak stresses, respectively, using the stress categorization results derived by classifying the loads acting during the seismic event, and then simply dividing the alternating stress by the elastic modulus, the following simplified elastic-plastic analysis procedure for strain-based fatigue assessment of nuclear safety class 1 component under the severe seismic loads can be obtained:

$$(\varepsilon_{alt})_{max} = S_{alt} / E \tag{5}$$

$$S_{alt} = 0.5(K_{se}S_{p\text{-}sb\text{-}sp} + K_{s\nu}K_{sn}S_{sb} + K_{s\nu}S_{sp}) \tag{6}$$

$$K_{se} = 1.0, \text{ for } S_n \le 3S_m$$

$$= 1.0+[(1\text{-}n)/n(m\text{-}1)]\times(S_n/3S_m\text{-}1)$$

$$\text{for } 3S_m < S_n < 3mS_m$$

$$= 1/n, \text{ for } S_n \ge 3mS_m \tag{7}$$

$$K_{s\nu} = 1.4, \text{ for } S_p > 3S_m \text{ and } S_{p\text{-}sb\text{-}sp} \ge 3S_m$$

$$= 1.0 + 0.4(S_p\text{-}3S_m)/(S_{sb+sp})$$

$$\text{for } S_p > 3S_m \text{ and } S_{p\text{-}sb\text{-}sp} < 3S_m$$

$$= 1.0, \text{ for } S_p \le 3S_m \tag{8}$$

$$\text{and } K_{s\nu} \le K_{se}$$

$$K_{sn} = 1.0+\{(S_{p\text{-}sp}/S_n)^{(1-n)/(1+n)}\text{-}1\}$$

$$\{(S_{p\text{-}sp}\text{-}3S_m)/S_{p\text{-}sp}\}, \text{ for } S_{p\text{-}sp} > 3S_m$$

$$= 1.0, \text{ for } S_{p\text{-}sp} \le 3S_m \tag{9}$$

$$\text{and } K_{sn}\times K_{s\nu} \le K_{se}$$

where $(\varepsilon_{alt})_{max}$ is the maximum total equivalent strain amplitude, which will be used for strain-based fatigue assessment of nuclear safety class 1 components subject to the severe seismic loads. E is elastic modulus. K_{se} is the penalty factor for primary stress and secondary membrane stress ranges caused by seismic anchor motion, $K_{s\nu}$ is the penalty factor that takes into consideration the Poisson's ratio effect for secondary local stress range caused by seismic anchor motion, K_{sn} is the penalty factor that considers the plastic strain redistribution effect in a notch for secondary bending stress range caused by seismic anchor motion. S_p is the total stress intensity range including deadweight, pressure, seismic inertia load, and seismic anchor motion, S_n is the total stress intensity range excluding peak stresses, which means range of primary plus secondary stress intensity, $S_{p\text{-}sb\text{-}sp}$ is the total stress intensity range excluding the secondary bending and secondary peak stresses due to seismic anchor motion, S_{sb} is the secondary bending stress intensity range due to seismic anchor motion, S_{sp} is the secondary peak stress intensity range due to seismic anchor motion, S_{sb+sp} is the secondary bending plus secondary peak stress intensity range due to seismic anchor motion, and $S_{p\text{-}sp}$ is the total stress intensity range excluding the secondary peak stresses due to seismic anchor motion.

3. Application of the stain-based simplified elastic-plastic analysis procedure

This section gives details of an application target. In addition, the dynamic FE time history elastic-plastic seismic analysis procedures and results performed to obtain a reference total strain amplitude value are presented. The application results of the strain-based simplified elastic-plastic analysis procedure to the target are presented. Finally, the fatigue assessment results using the calculated total strain amplitude and the strain-based acceptance criteria are presented.

3.1. Application example

A hot leg surge nozzle in pressurizer surge line was selected as the application target. Fig. 1 shows a schematic configuration of the target. The pressurizer lower head, hot leg reactor coolant piping and, surge nozzle are made of low alloy steel, SA 508 Gr.3 Cl.1, and the safe end and surge line piping are made of austenitic stainless steel, SA 312 TP316. The surge line is supported by three snubbers S1Z, S2Y, and S3X, a sway strut R1Z and a pressurizer skirt, and connected to the hot leg at the hot leg surge nozzle.

Table 1 presents physical and mechanical properties including elastic modulus, density, Poisson's ratio, mechanical strengths, and

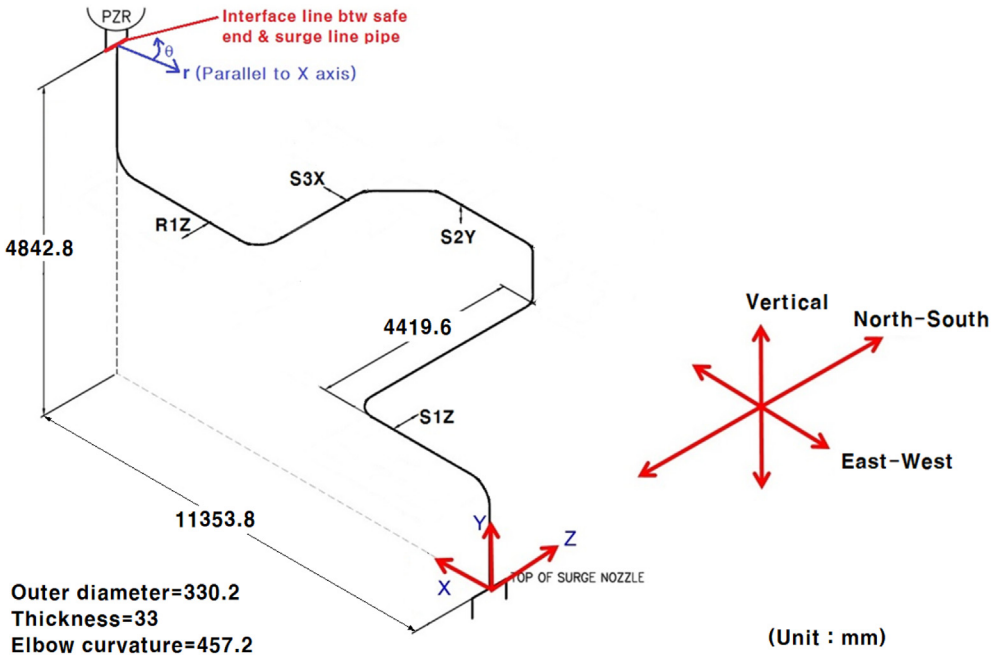

(a)

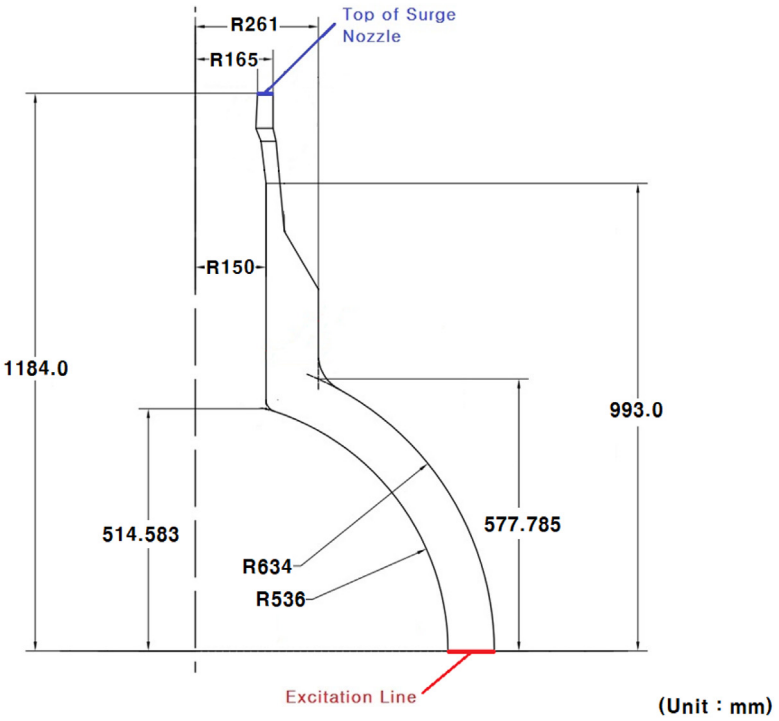

(b)

Fig. 1. Schematic configuration of the pressurizer surge line and the hot leg surge nozzle: (a) pressurizer surge line and (b) hot leg surge nozzle.

uniform elongation of the materials at 316 °C [22,23]. The Chaboche hardening model was utilized in the study [24]. Table 2 presents Chaboche combined hardening model parameters of the materials at 316 °C [23]. Density of reactor coolant at 316 °C and 15 MPa is assumed to be 0.69 g/cm3 [25].

Seismic loads corresponding to peak ground acceleration (PGA) 0.6 g and 1.2 g were applied to supports the supports in Fig. 1 (R1Z, S3X, S2Y, S1Z). The PGA 0.6 g is twice the PGA 0.3 g corresponding to SSE of South Korea nuclear power plants. Fig. 2 depicts displacement time histories at the supports by the seismic inertia corresponding to 0.6 g. E-W and N-S mean east-west and north-south, respectively. The displacement time histories do not include the seismic anchor motions presented in Fig. 3. The target is subject to inner pressure, 15 MPa.

Table 1
Physical and mechanical properties of SA 508 Gr.3 Cl.1 and SA 312 TP316 at 316 °C.

Material	SA508 Gr.3 Cl.1	SA312 TP316
Elastic modulus	184.1 GPa	175.4 GPa
Density	7.75 g/cm^3	8.03 g/cm^3
Poisson's ratio	0.3	0.31
Yield strength	427.5 MPa	155.6 MPa
Ultimate tensile strength	620.1 MPa	455.4 MPa
Uniform elongation	0.112 mm/mm	0.325 mm/mm

A hybrid FE model consisting of continuum and beam elements, shown in Fig. 4, was used. Continuum elements were applied to areas where plasticity is expected to occur due to high stress and strain, and beam elements were applied to areas expected to have elastic behavior.

3.2. Dynamic FE time history elastic-plastic seismic analysis

Dynamic FE time history elastic-plastic seismic analysis was carried out using an implicit version of a commercial FEA program, ABAQUS [26] and the Chaboche combined hardening model. Nonlinear geometric option was applied to consider large deformation effect. Automatic time increment control was used, having the maximum time increment, 0.005 s, equal to time increment of the displacement time histories. In performing dynamic FE elastic-plastic analysis, the total displacement histories calculated by linearly combining the seismic inertia displacements in Fig. 2 and the seismic anchor motion displacements in Fig. 3 were used. In the analysis for PGA 1.2 g, the displacement time histories were determined by doubling the displacement time histories of PGA 0.6 g.

Fig. 5 shows the total equivalent strain distribution corresponding to 0.6 g at the time of occurrence of the maximum value (11.51 s). As shown in the figure, it can be seen that the maximum total equivalent strain occurs at the outer surface in safety end of the hot leg nozzle. In addition, the maximum value occurs at 159° counterclockwise with respect to the positive x-axis. The point was selected as the fatigue assessment point.

Fig. 6 shows the time history of each total strain component at the maximum total equivalent strain generation location. ε_{xx}, ε_{yy}, and ε_{zz} represent the normal strains in the axial directions given in each subscript. ε_{xy}, ε_{yz}, and ε_{zx} represent the shear strains in the axial directions given in each subscript. These strain components were utilized as input data for the fatigue assessment.

3.3. Application of the strain-based simplified elastic-plastic analysis procedure

Static FE elastic stress analysis was performed separately for the deadweight, the pressure, and the seismic anchor motions using the ABAQUS. In addition, dynamic FE elastic seismic analysis was carried out for the seismic inertia loads using the ABAQUS. In order to calculate the penalty factors such as K_e, K_n, and K_v from the FEA results, the strain-based simplified elastic-plastic analysis procedure proposed in subsection 2.2 was utilized.

Table 3 presents application results of the strain-based simplified elastic-plastic analysis procedure. From the table, it is identified that all the penalty factors for the PGA 0.6 g are less than 1.9 whereas the K_e for the PGA 1.2 g are greater than 3.0, and the maximum total equivalent strain amplitude is 0.2549% and 0.8713% for PGA 0.6 g and 1.2 g, respectively.

Table 2
Chaboche combined hardening model parameters of SA 508 Gr.3 Cl.1 and SA 312 TP316 at 316 °C.

SA 508 Gr.3 Cl.1	Isotropic hardening parameters	Q (MPa)					b		
		220					0.5		
	Kinematic hardening parameters	σ0 (MPa)	C_1 (MPa)		γ_1	C_2 (MPa)	γ2	C_3 (MPa)	γ3
		222	210000		2000	42000	400	5500	10
SA 312 TP316	Isotropic hardening parameters	Q (MPa)					b		
		143.4					20.9		
	Kinematic hardening parameters	σ0 (MPa)	C_1 (MPa)	γ_1		C_2 (MPa)	γ2	C_3 (MPa)	γ3
		99.2	90800	927		15690	1365	5310	1

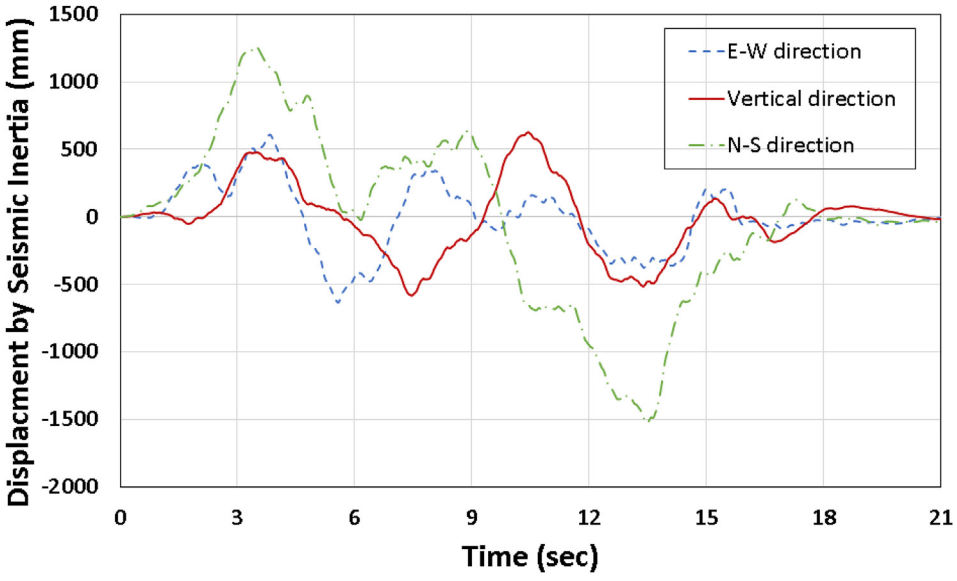

Fig. 2. Displacement time histories at the supports of the pressurizer surge line by the seismic inertia corresponding to 0.6 g.

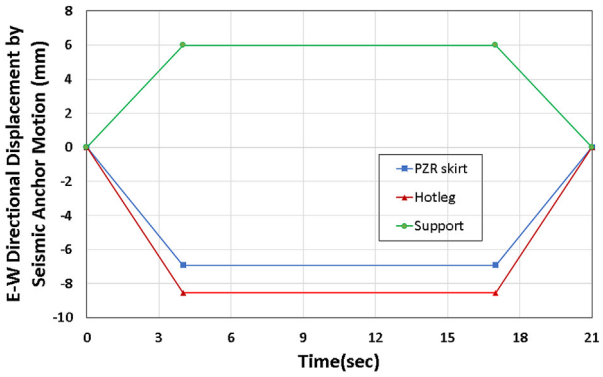

(a)

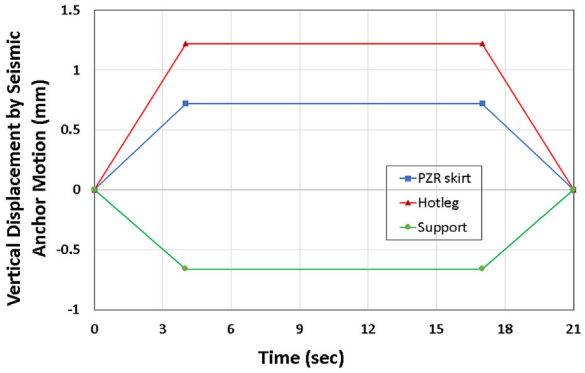

(b)

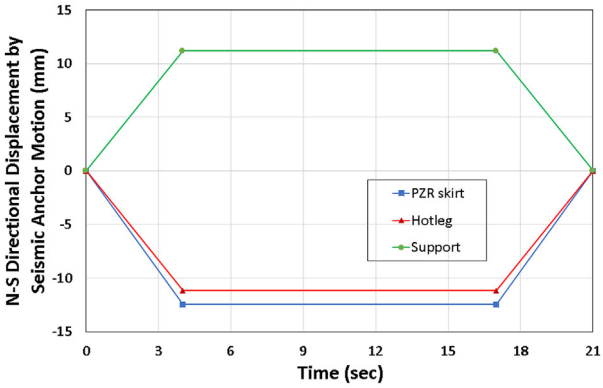

(c)

Fig. 3. Displacement time histories at the supports of the pressurizer surge line by the seismic anchor motion corresponding to 0.6 g: (a) E-W direction, (b) vertical direction, and (c) N-S direction.

4. Fatigue assessment

This section compares the strain-based fatigue assessment procedure of the ASME B&PV Code, Sec.III, Subsec.NB, Article NB-3200 [3] with the one of the ASME B&PV Code, Sec.III, Code Case Nxxx [17]. In this section, a strain-based fatigue assessment procedure is proposed based on the comparison result. In addition, this section presents the fatigue assessment results using the detail FE elastic-plastic seismic analysis and the simplified elastic-plastic analysis.

4.1. Strain-based fatigue assessment procedure

The 1994 version of the ASME B&PV Code, Sec.III, Subsec.NB, NB-3200 presented the following strain-based acceptance criteria:

Fig. 4. Hybrid FE model of the pressurizer surge line.

$$(\varepsilon_{alt})_{max} < S_a(N)/(E \cdot N^{0.5}) \quad (10)$$

where $S_a(N)$ is an allowable stress amplitude for N cycles of load and can be obtained from Figure I-9.1 or I-9.2 of the ASME B&PV Code, Sec.III Appendices, Mandatory Appendix I [27]. N is number of cycles of dynamic load.

The ASME B&PV Code, Sec.III, Code Case Nxxx specifying alternative rules for the level D service limits proposes the following strain-based acceptance criteria for reversing dynamic loads not required to be combined with non-reversing dynamic loads:

$$(TF) \cdot (\varepsilon_{eq})_{max} \leq S_a(N)(a/E) \quad (11)$$

$$TF = (\sigma_1 + \sigma_2 + \sigma_3)/\ \sigma_{von} \quad (12)$$

where $(\varepsilon_{eq})_{max}$ is a maximum equivalent strain, TF is a triaxiality factor and a is a factor to adjust the fatigue curves of Appendix I to obtain a factor of safety of 2 against failure. The "a" factor has a value of 2.3 for carbon steel and one of 1.5 for austenitic steel [17]. σ_1, σ_2, *and* σ_3 are principal stresses, and σ_{von} is a von Mises effective stress.

From the above summary results, it can be found that both procedures use strains. The former lowers the acceptance criteria value by dividing a stress amplitude of the specific fatigue cycle by a square root of the corresponding number of cycles, while the latter considers the triaxiality factor and the fatigue curve adjustment factor. That is, the former does not consider the triaxility factor. The triaxiality factor may greatly vary over time during seismic loads. Also, because the von Mises effective stress is located in the denominator of the factor, it is very sensitive to FE model and analysis procedure. Seismic loads are representative non-proportional loads. There is very little research on how to determine the representative triaxiality factor. The latter does not provide any procedure for determining the triaxiality factor. The former is much simpler than the latter because of not considering the triaxiality factor. For this reason, the former is much easier to apply and has much less uncertainty in analysis than the latter. Based on these review results, the procedure presented in the 1994 version of the ASME B&PV Code, Sec.III, Subsec.NB, NB-3200 was utilized as a strain-based fatigue assessment procedure for the present study. The fatigue cycle number, N was considered in two cases, 10 cycles and 20 cycles.

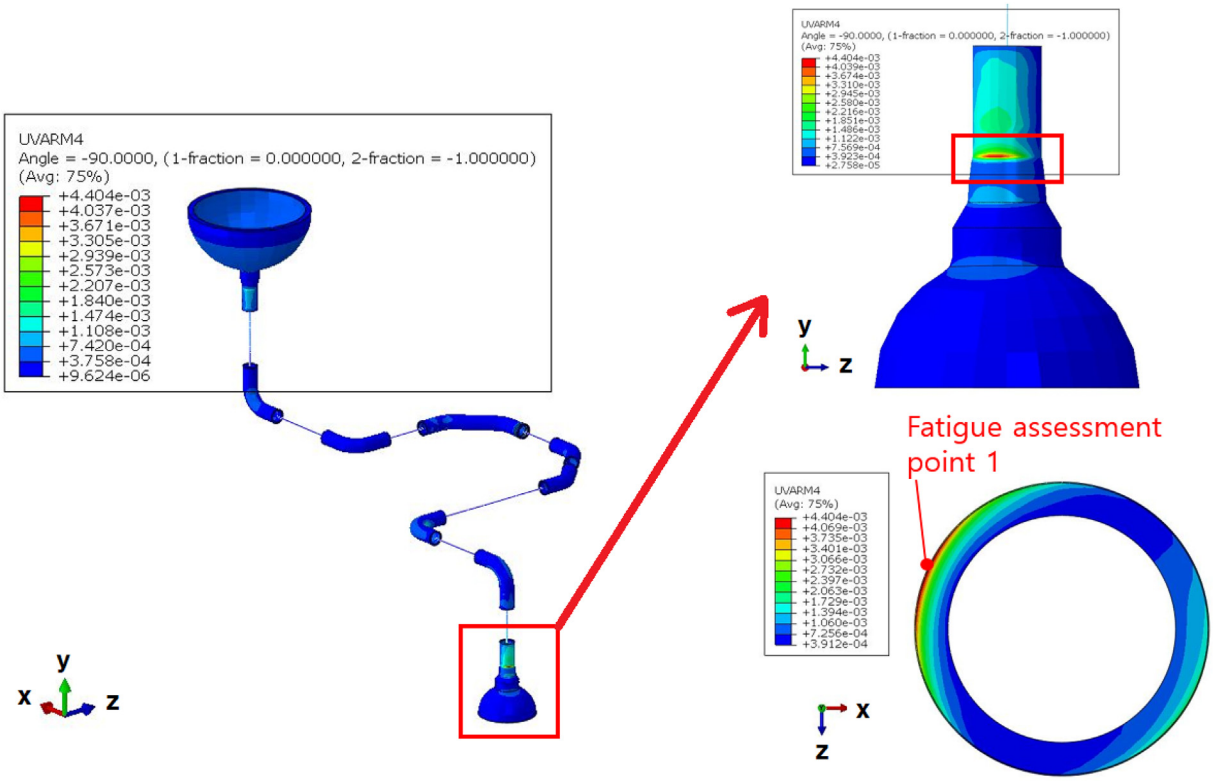

Fig. 5. Total equivalent strain distribution corresponding to 0.6 g at the time of occurrence of the maximum value (11.51 s).

4.2. Fatigue assessment results

For the strain-based fatigue assessment using the dynamic FE time history elastic-plastic analysis results, maximum total equivalent strain amplitude was calculated from the total strain histories presented in Fig. 6 as follows:

$$(\varepsilon_{alt})_{max} = 1/(3\sqrt{2})[(\Delta\varepsilon_{xx}-\Delta\varepsilon_{yy})^2+(\Delta\varepsilon_{yy}-\Delta\varepsilon_{zz})^2+(\Delta\varepsilon_{zz}-\Delta\varepsilon_{xx})^2+1.5(\Delta\varepsilon^2_{xy}+\Delta\varepsilon^2_{yz}+\Delta\varepsilon^2_{zx})]^{0.5} \quad (13)$$

where, Δ means increment of the corresponding total strain component at the times at which the maximum and minimum values of the total equivalent strain were derived considering direction of the maximum total principal strain.

Table 4 presents the maximum total equivalent strain amplitudes calculated using the dynamic FE time history elastic-plastic analysis results. Table 5 presents the fatigue assessment results using the dynamic FE time history elastic-plastic analysis result. From these tables, it can be found that the maximum total equivalent strain amplitudes are 0.2439% and 0.5782% for PGA 0.6 g and 1.2 g, respectively. In addition, the strain-based criteria are satisfied for all cases.

The fatigue assessment results using the strain-based simplified elastic-plastic analysis procedure are presented in Table 6. From the table, it is identified that the case of PGA 1.2 g and $N = 20$ cycles is not satisfied with the strain-based criteria whereas the other cases are satisfied.

5. Comparisons and discussions

The comparison results are presented in Table 7, showing reasonable good agreement between the detailed FE elastic-plastic seismic analysis results and the simplified elastic-plastic analysis results. From the table, it is found that the simplified elastic-plastic analysis procedure yields the maximum total equivalent strain amplitude value that is about maximum 50.7% larger than the detailed FE elastic-plastic seismic analysis, and the excess degree of the simplified elastic-plastic analysis procedure increases with increasing the PGA. The safety margin for PGA 0.6 g is similar in both the analyses, indicating that the simplified elastic-plastic analysis procedure yields a slightly conservative evaluation results. In addition, it can be seen from the safety margin for the PGA 1.2 g that the conservatism of the simplified elastic-plastic analysis procedure increases. The reason is that the stress components not only almost linearly increase about 2 times, but the K_e factor also increases from 1.879 to 3.333 when the PGA is doubled from 0.6 g to 1.2 g as shown in Table 3. Eventually, it can be determined that the strain-based simplified elastic-plastic analysis procedure was valid from the viewpoint of conservative assessment, which is very important for design of nuclear safety-related components.

In general, the FE elastic-plastic seismic analysis requires many input data and is sensitive to such input data. So, it can be difficult for nuclear industries to apply the FE elastic-plastic seismic analysis to design of nuclear components from the viewpoint of engineering application. On the contrary, the simplified elastic-plastic analysis procedures using elastic analysis results are relatively easier to apply to the design. It is recommended that the simplified elastic-plastic analysis procedure be applied to the design because it results in reasonably conservative results as well as its ease in application.

6. Conclusions

By performing the study about simplified elastic-plastic analysis applicable to seismic design of nuclear safety class 1 components under the severe seismic loads, the following conclusions were

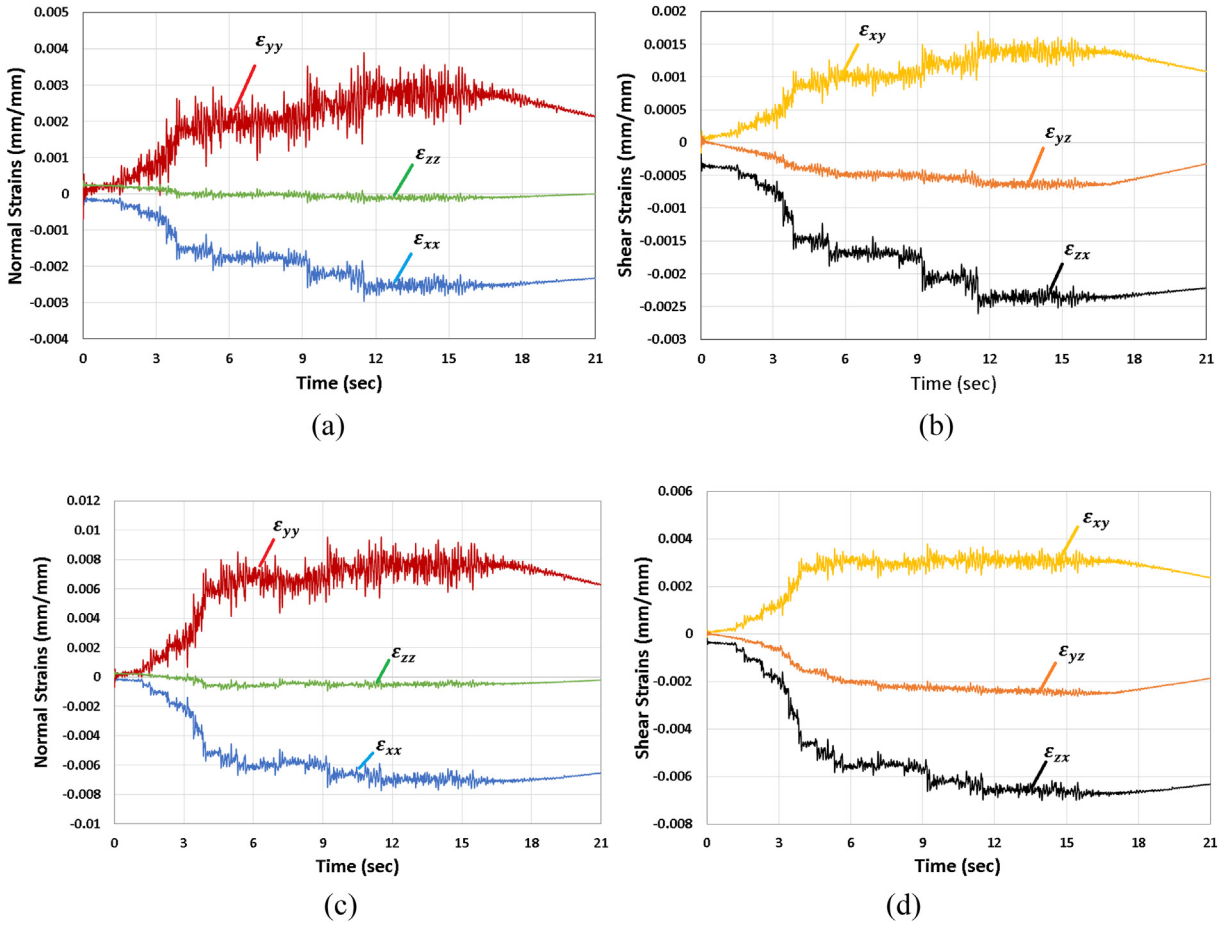

Fig. 6. Total strain histories at the maximum total strain generation location: (a) normal strains (0.6 g), (b) shear strains (0.6 g), (c) normal strains (1.2 g), and (d) shear strains (1.2 g).

Table 3
Maximum total equivalent strain amplitudes calculated by applying the strain-based simplified elastic-plastic analysis procedure.

N			m			E (MPa)			S_m (MPa)			
0.30			1.70			175,400			117.08			
PGA (g)	S_n (MPa)	S_p (MPa)	$S_{p\text{-}sb\text{-}sl}$ (MPa)	S_{sb+sl} (MPa)	$S_{p\text{-}sl}$ (MPa)	S_{sb} (MPa)	S_{sl} (MPa)	K_{se}	K_{sp}	K_{sn}	S_{alt} (MPa)	$(\varepsilon_{alt})_{max}$ (%)
0.6	443.9	488.6	434.7	54.4	478.8	44.6	10.2	1.879	1.4	1.011	447.1	0.2549
1.2	887.7	977.2	869.3	108.9	957.5	89.2	20.4	3.333	1.4	1.041	1528.2	0.8713

Table 4
Maximum total equivalent strain amplitudes calculated using the dynamic FE time history elastic-plastic seismic analysis results.

PGA (g)	Max./Min.	Time (sec)	ε_{xx} (%)	ε_{yy} (%)	ε_{zz} (%)	ε_{xy} (%)	ε_{yz} (%)	ε_{zx} (%)	$(\varepsilon_{alt})_{max}$ (%)
0.6	Maximum	11.52	−0.2962	0.3891	−0.0274	0.1694	−0.0509	−0.2608	0.2439
	Minimum	0.005	0.0158	−0.0690	0.0367	−0.0156	−0.0019	−0.0176	
1.2	Maximum	11.52	−0.7733	0.9537	−0.0812	0.3674	−0.2187	−0.6978	0.5782
	Minimum	0.005	0.0157	−0.0688	0.0366	−0.0155	−0.0019	−0.0177	

Table 5
The strain-based fatigue assessment results using the dynamic FE time history elastic-plastic seismic analysis results.

PGA (g)	Max. total equivalent strain $(\varepsilon_{eq})_{max}$ (%)	Elastic modulus E (MPa)	Allowable stress amplitude $S_a(N)$ (MPa)		Acceptance criteria value $S_a(N)/(E{\cdot}N^{0.5})$ (%)		Safe/Fail	
			N = 10 cycles	N = 20 cycles	N = 10 cycles	N = 20 cycles	N = 10 cycles	N = 20 cycles
0.6	0.2439	195,000	6000	4800	0.973	0.778	Safe	Safe
1.2	0.5782	195,000	6000	4800	0.973	0.778	Safe	Safe

Table 6
The strain-based fatigue assessment results using the strain-based simplified elastic-plastic analysis procedure.

PGA (g)	Max. total equivalent strain $(\varepsilon_{eq})_{max}$ (%)	Elastic modulus E (MPa)	Allowable stress amplitude $S_a(N)$ (MPa)		Acceptance criteria value $S_a(N)/(E{\cdot}N^{0.5})$ (%)		Safe/Fail	
			N = 10 cycles	N = 20 cycles	N = 10 cycles	N = 20 cycles	N = 10 cycles	N = 20 cycles
0.6	0.2549	195,000	6000	4800	0.973	0.778	Safe	Safe
1.2	0.8713	195,000	6000	4800	0.973	0.778	Safe	Fail

Table 7
Comparison of the maximum total equivalent strain amplitude and the fatigue assessment results between the simplified elastic-plastic analysis and the detailed FE elastic-plastic seismic analysis.

Analysis method		Max. total equivalent strain $(\varepsilon_{eq})_{max}$ (A) (%)	Acceptance criteria value $S_a(N)/(E{\cdot}N^{0.5})$ (B) (%)		Safety margin[Note)] (C) (%)	
			N = 10 cycles	N = 20 cycles	N = 10 cycles	N = 20 cycles
Detailed FE elastic-plastic seismic analysis	0.6 g	0.2439	0.973	0.778	74.93	68.65
	1.2 g	0.5782	0.973	0.778	40.58	20.53
Simplified elastic-plastic analysis	0.6 g	0.2549	0.973	0.778	73.80	67.24
	1.2 g	0.8713	0.973	0.778	10.45	−11.99

Note) C = 100 x (B-A)/B.

derived:

A simplified elastic-plastic analysis procedure for strain-based fatigue assessment is proposed to evaluate structural integrity of nuclear safety class 1 components subject to severe seismic loads,

In case of the hot leg surge nozzle, as comparing with the detailed FE elastic-plastic seismic analysis, the proposed simplified elastic-plastic analysis procedure can be recommended as a suitable procedure to be applied at the desig[1–27] n because of the reasonably conservative results and ease of application.

Declaration of competing interest

The authors declare that they have no known competing financial interests or personal relationships that could have appeared to influence the work reported in this paper.

Acknowledgment

This work was supported by Korea Institute of Energy Technology Evaluation and Planning (KETEP) (No. 20171520101650, No. 20181510102380).

References

[1] ASME Boiler and Pressure Vessels Code Committee, ASME B&PV Code, Section III: Rules for Construction of Nuclear Facility Components, 2019.
[2] G.R. Reddy, Hari Prasad Muruva, Ajit Kumar Verma, Textbook of Seismic Design: Structures, Piping Systems, and Components, Springer, 2019.
[3] ASME Boiler and Pressure Vessels Code Committee, ASME B&PV Code, Section III, Subsection NB, Article NB-3200, 1994.
[4] https://www.powertechnology.com/projects/kashiwazaki/.
[5] https://www.worldnuclear.org/information-library/safety-and-security/safety-of- plants/fukushima-accident. aspx.
[6] US NRC, Recommendations for Enhancing Reactor Safety in the 21st Century: the Near Term Task Force Review of Insights from, Fukushima Dai-Ichi Accident, 2011.
[7] NSC, Regulatory Guide for Reviewing Seismic Design of Nuclear Power Reactor Facilities, NSCRG-1-DS-1.02, 2006.
[8] IAEA, Considerations on the Application of the IAEA Safety Requirements for the Design of Nuclear Power Plants, IAEA-TECDOC-1791, 2016.
[9] ASME Boiler & Pressure Vessels Code Committee. Task Group for Evaluation of beyond Design Basis Events (BPV XI).
[10] ASME Boiler & Pressure Vessels Code Committee. KIWG Task Group on Elasto-Plastic Analysis Based Seismic Evaluations.
[11] Izumi Nakamura, Naoto Kasahara, Excitation tests on elbow pipe specimens to investigate failure behavior under excessive seismic loads, in: Proceedings of ASME PVP 2015. PVP2015-45711, 2015, 2015 July 19-23.
[12] OECD NEA, Integrity of Structures, Systems and Components under Design and beyond Design Loads in Nuclear Power Plants: Final Report of the Project on Metallic Component Margins under High Seismic Loads (MECOS). NEA/CSNI/R 3 (2018), 2018.
[13] US NRC, Seismic Analysis of Large-Scale Piping Systems for the JNES-NUPEC Ultimate Strength Piping Test Program, NUREG/CR-6983, 2008.
[14] Izumi Nakamura, Akihito Otani, Masaki Morishita, Seismic qualification of piping systems by detailed inelastic response analysis: part 3 - variation in elastic-plastic analysis results on carbon steel pipes from the benchmark analyses and the parametric analysis, in: Proceedings of ASME PVP 2017. PVP2017-65316, 2017, 2017 July 16-20.
[15] Tomoyoshi Watakabe, Izumi Nakamura, Akihito Otani, Masaki Morishita, Tadahiro Shibutani, Masaki Shiratori, Seismic qualification of piping systems by detailed inelastic response analysis: part 4 – second round benchmark analyses with stainless steel piping component test, in: Proceedings of ASME PVP 2017. PVP2017-65324, 2017, 2017 July 16-20.
[16] JSME, Codes for Nuclear Power Generation Facilities – Rules on Design and Construction for Nuclear Power Plant: Alternative Design for Seismic Design of Seismic S Class Steel Piping Based on Elastic-Plastic Response Analysis, NC-CC-008, 2019.
[17] ASME Boiler & Pressure Vessels Code Committee, ASME B&PV Code, Sec.III, Div.1, Code Case Nxxx: Alternative Rules for Level D Service Limits of Class 1, 2, and 3 Piping Systems, 2019. Technical Basis for Code Cans Nxxx: Alternative Rules for Level D Service Limits of Class 1, 2, and 3 Piping Systems. Technical Basis Documents for Record #13-1438, 2019.
[18] ASME Boiler & Pressure Vessels Code Committee, ASME B&PV Code, Sec.III, Div.1, Code Case N-779: Alternative Rules for Simplified Elastic-Plastic Analysis Class, vol. 1, 2009.
[19] Jong-Sung Kim, Jae-Wook Jeong, Kang-Yong Lee, Proposal of the penalty factor equations considering weld strength over-match, Nucl. Eng. Technol. 49 (2017) 838–849, 49(4).
[20] Argonne National Laboratory, Review of the Margin for ASME Code Fatigue Design Curve – Effects of Surface Roughness and Material Variability, NUREG/CR-6815, 2003.
[21] ASME Boiler and Pressure Vessels Code Committee, ASME B&PV Code, Section III, Subsection NB, Article NB-3228.5, Simplified Elastic-Plastic Analysis, 2019, 2015.
[22] ASME Boiler and Pressure Vessels Code Committee, ASME B&PV Code, Section II, Part D: Properties Materials, 2019.
[23] G.H. Koo, Inelastic Material Model for Type 316H, ASME BPV III Colorado Springs Meeting Task Group on Inelastic Analysis Methods, 2015.
[24] J.L. Chaboche, Constitutive equations for cyclic plasticity and cyclic visco-plasticity, Int. J. Plast. 5 (Iss.3) (1989) 247–302.
[25] https://www.steamtablesonline.com/steam 97web.aspx.
[26] Dassault Systems, ABAQUS Version 6.16. User's Manuals, 2016.
[27] ASME Boiler and Pressure Vessels Code Committee, ASME B&PV Code, Section III, Appendices, Mandatory Appendix I, 2019.